Atmospheric Pressure Laser-Induced Acoustic Desorption Chemical Ionization Mass Spectrometry for Analysis of Saturated Hydrocarbons

ARTICLE *in* ANALYTICAL CHEMISTRY · AUGUST 2012

Impact Factor: 5.64 · DOI: 10.1021/ac301307p · Source: PubMed

6 AUTHORS, INCLUDING:

Chang S Hsu
Florida State University
151 PUBLICATIONS **1,672** CITATIONS

SEE PROFILE

analytical chemistry

Article

pubs.acs.org/ac

Atmospheric Pressure Laser-Induced Acoustic Desorption Chemical Ionization Mass Spectrometry for Analysis of Saturated Hydrocarbons

Leonard Nyadong,[†] John P. Quinn,[†] Chang S. Hsu,[§] Christopher L. Hendrickson,[†,‡,§] Ryan P. Rodgers,*[,†,‡,§] and Alan G. Marshall*[,†,‡,§]

[†]National High Magnetic Field Laboratory, Florida State University, 1800 East Paul Dirac Drive, Tallahassee, Florida 32310, United States

[‡]Department of Chemistry and Biochemistry, Florida State University, 95 Chieftain Way, Tallahassee, Florida 32303, United States

[§]Future Fuels Institute, Florida State University, 1800 East Paul Dirac Drive, Tallahassee, Florida 32310, United States

Supporting Information

ABSTRACT: We present atmospheric pressure laser-induced acoustic desorption chemical ionization (AP/LIAD-CI) with O_2 carrier/reagent gas as a powerful new approach for the analysis of saturated hydrocarbon mixtures. Nonthermal sample vaporization with subsequent chemical ionization generates abundant ion signals for straight-chain, branched, and cycloalkanes with minimal or no fragmentation. $[M - H]^+$ is the dominant species for straight-chain and branched alkanes. For cycloalkanes, $M^{+\bullet}$ species dominate the mass spectrum at lower capillary temperature (<100 °C) and $[M - H]^+$ at higher temperature (>200 °C). The mass spectrum for a straight-chain alkane mixture (C_{21}−C_{40}) shows comparable ionization efficiency for all components. AP/LIAD-CI produces molecular weight distributions similar to those for gel permeation chromatography for polyethylene polymers, Polywax 500 and Polywax 655. Coupling of the technique to Fourier transform ion cyclotron resonance mass spectrometry (FTICR MS) for the analysis of complex hydrocarbon mixtures provides unparalleled mass resolution and accuracy to facilitate unambiguous elemental composition assignments, e.g., 1754 peaks (rms error = 175 ppb) corresponding to a paraffin series (C_{12}−C_{49}, double-bond equivalents, DBE = 0) and higher DBE series corresponding to cycloparaffins containing one to eight rings. Isoabundance-contoured plots of DBE versus carbon number highlight steranes (DBE = 4) of carbon number C_{27}−C_{30} and hopanes of C_{29}−C_{35} (DBE = 5), with sterane-to-hopane ratio in good agreement with field ionization (FI) mass spectrometry analysis, but performed at atmospheric pressure. The overall speciation of nonpolar, aliphatic hydrocarbon base oil species offers a promising diagnostic probe to characterize crude oil and its products.

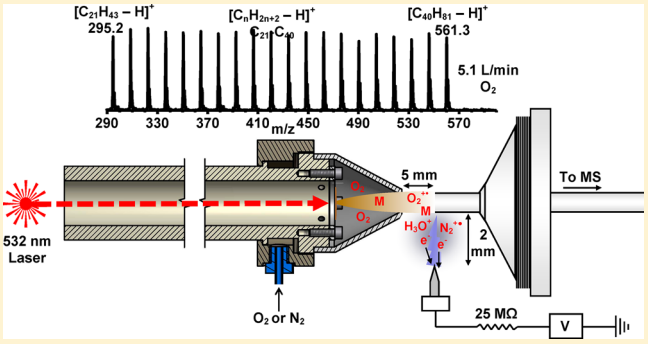

Saturated hydrocarbons, a major fraction in most petroleum crude oils, present a challenge for mass spectrometry analysis because of their lack of easily ionizable functional groups and tendency to fragment. They have most commonly been analyzed by use of vacuum-based techniques such as electron ionization (EI),[1] field ionization (FI), and field desorption (FD).[2−4] However, the high-energy electrons (70 eV) used in EI often result in exhaustive fragmentation of the molecular ion. The use of a supersonic molecular beam to vibrationally cool the gas-phase analytes prior to EI can reduce (but not eliminate) fragmentation, which can be further decreased by use of lower-energy electrons (18 eV).[5,6] Jet cooling of laser-desorbed analytes followed by vacuum ultraviolet (VUV) single-photon photoionization to generate saturated hydrocarbon molecular ions has also been reported.[7] Nevertheless, FI and FD are the main soft ionization techniques currently used for saturated hydrocarbon analysis. For FI/FD, the thermal vaporization/heating of a sample can also cause fragmentation of the high-boiling paraffins, especially branched paraffins, which can result in almost complete dissociation of the molecular ion.[8] Direct laser desorption/ionization (LDI) techniques with various transition metal reagent cations (e.g., Ag^+, Cu^+, Mn^+, and Cr^+) have also shown promise for the analysis of saturated hydrocarbons.[9,10] However, LDI methods often discriminate against higher-mass species that can either undergo dissociation to generate abundant lower-mass fragment ions or aggregate with other species in the desorption plume.[10] Atmospheric pressure ionization techniques recently shown to generate saturated hydrocarbon molecular ion and/or hydride abstraction signals include direct analysis in real time[11]

Received: May 30, 2012
Accepted: July 24, 2012
Published: August 6, 2012

and a helium plasma ionization source (HPIS),[12] both of which require thermal vaporization of the sample. However, those techniques exhibit low- and high-mass discrimination and the high thermal energy required to vaporize the high-boiling alkanes readily induces dissociation, especially for branched alkanes. Desorption electrospray ionization (DESI) in the presence of an electric discharge has also been used for the analysis of saturated hydrocarbons.[13] This method results in a complex mass spectrum in which each saturated hydrocarbon species generates multiple alcohol and hydroxyketone oxidation products and no unoxygenated hydrocarbon signal. The use of paraffinic solvents (e.g., *n*-pentane and *n*-hexane) for atmospheric pressure chemical ionization of saturated hydrocarbons with minimal fragmentation has also been reported.[14,15]

Laser-induced acoustic desorption (LIAD) is a technique for vaporization of analytes from a thin metal foil by use of acoustic waves generated in the foil following laser irradiation from the side opposite the deposited sample.[16−19] Gas-phase neutrals are generated by this technique with little or no internal energy deposition.[20] Ionization can thus be tailored to generate intact analyte ions with little or no fragmentation. LIAD has been coupled to chemical ionization in vacuum by use of a complex series of reactions to generate a cyclopentadienyl cobalt radical cation, for efficient desorption/ionization of saturated hydrocarbons with little or no fragmentation[21,22] and no bias between low-mass and high-mass species. The technique yields molecular weight distributions similar to those from gel permeation chromatography (GPC) for low-mass polyethylene.[22] A ligated water cluster of Mn^+ (namely, $ClMn(H_2O)^+$) has also been coupled with LIAD as a chemical ionization reagent in vacuum for the analysis of the saturated hydrocarbons in base oil.[23] LIAD has also recently been coupled to a synchrotron VUV photoionization source for the analysis of heavy oils.[24]

We recently coupled LIAD with CI at atmospheric pressure to a Fourier transform ion cyclotron resonance mass spectrometer (FTICR MS) to demonstrate the advantages of atmospheric pressure implementation for the analysis of polar and nonpolar polyaromatic components of a petroleum distillate.[25] Here we extend application of this technique to the analysis of saturated hydrocarbons, including straight-chain, branched-chain, and cycloparaffins, with little or no fragmentation by use of a modified sample probe with O_2 reagent/carrier gas. We apply the method to (1) analysis of polyethylene to yield molecular weight distributions similar to those from GPC and (2) analysis of a complex saturated hydrocarbon mixture (base oils) with molecular weight distribution nearly identical to that from FD/FI, but superior to FI with respect to throughput, cost, and robustness afforded by atmospheric pressure implementation.

EXPERIMENTAL METHODS

Reagents and Samples. All reagents and samples were used without additional purification. HPLC grade toluene (99.9%, Sigma-Aldrich, St. Louis, MO, U.S.A.) was used for sample dissolution and dilution. Ion source optimization and characterization experiments were performed by use of the following saturated hydrocarbon model compounds: triacontane, tricosane, hexatriacontane, squalane, 5-α cholestane, alkane mixture C_{21}−C_{40}, Polywax 500, and Polywax 655, purchased from Sigma-Aldrich. The optimized method was applied to analysis of a premium base oil sample. Ultrapure carrier grade O_2 (99.996%, OX UPC 300, Airgas South, Inc., Tallahassee, FL) and BIP technology grade N_2 (99.9999%, NI BIP300) were used as carrier/reagent gases.

AP/LIAD-CI Ion Source. A previously described atmospheric pressure laser-induced acoustic desorption chemical ionization (AP/LIAD-CI) FTICR MS interface[25] was modified for this study. The ion source was coupled to a 9.4 T FTICR and a linear ion trap mass spectrometer through a reconfigured Thermo Finnigan (San Jose, CA, U.S.A.) APCI source. The sample probe was modified to provide a pathway for introduction and confinement of the flow of reagent gas and vaporized analytes. The probe consists of a hollow PEEK cylinder (131 mm long, 11 mm i.d., 18.4 mm o.d., Upchurch Scientific, Oak Harbor, WA, U.S.A.) and a screw-on PEEK fitting on one end (14 mm long, 18.4 mm i.d., 31 mm o.d.) to create a small volume for directed carrier/reagent gas introduction (Figure 1, top, left). Additional details of the new probe are presented in the Supporting Information.

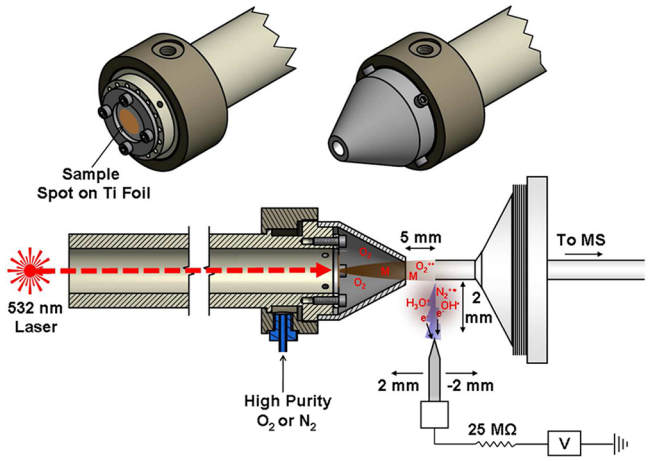

Figure 1. Schematic diagram of the AP/LIAD-CI source interfaced to a linear ion trap mass spectrometer. The source was also coupled to a 9.4 T FTICR mass spectrometer in the same configuration.

Sample Preparation for AP/LIAD-CI. A stock solution (10 mM) of each saturated hydrocarbon model compound in toluene was diluted to 1 mM for characterization experiments. The polywax and base oil samples were diluted to 1 mg/mL prior to analysis, and the standard alkane mixture (C_{21}−C_{40}) was spotted as received. An amount of 2 μL of each sample was spotted onto the Ti foil. After solvent evaporation the stainless steel cone was mounted and the cone-to-MS distance adjusted to ∼5 mm unless stated otherwise. The gas flow and the discharge were turned on for ∼10−30 s followed by laser irradiation of the back side of the foil. LIAD-vaporized neutrals are entrained by the carrier gas and swept toward the MS inlet, where they are ionized by reaction with reagent ions generated from the carrier by corona discharge.

Linear Ion Trap Mass Spectrometry (LIT MS). All ion source optimization and characterization experiments were performed with an LIT mass analyzer (LTQ, Thermo Finnigan, San Jose, CA, U.S.A.) equipped with automatic gain control. Typical instrument parameters were as follows: capillary voltage, 50 V; capillary temperature, 150 °C (unless stated otherwise); tube lens voltage, 25 V. Data were acquired and processed by use of Xcalibur version 2.0 software (Thermo Fisher Scientific, San Jose, CA, U.S.A.). Each mass spectral scan

dx.doi.org/10.1021/ac301307p | *Anal. Chem.* 2012, 84, 7131−7137

consisted of three microscans, 100 ms maximum ion injection period. All experiments were performed with positive ions.

9.4 T FTICR Mass Spectrometry and Data Analysis. The polyethylene and base oil samples were analyzed with a custom-built 9.4 T FTICR mass spectrometer. AP/LIAD-CI-generated ions traverse a heated metal capillary into a first octopole trap, in which the ions are accumulated for a very short period (70 ms). The ions are then transferred through a quadrupole ion guide to a second octopole trap, in which they are further accumulated for a total of 20 injections from the first octopole. Ultrapure carrier grade helium gas (99.9995%, Air Gas South Inc., Tallahassee, FL) was introduced into the second octopole to collisionally cool the ions prior to transfer through a set of rf-only quadrupole ion guides (120 cm total length) into an open cylindrical ion trap (9.4 cm i.d., 30 cm long).[26] The ions were cyclotron-excited by broad-band frequency sweep (chirp) excitation and were subsequently detected as the differential current induced between two opposed electrodes of the ICR cell. For each AP/LIAD-CI MS experiment 1−15 digitized time-domain ICR transients, corresponding to 10−150 laser shots, were collected and averaged,[27] with the LIAD probe manually rotated at ∼7 rpm about its longitudinal axis during data acquisition. Each of the acquisitions was Hanning-apodized and zero-filled prior to fast Fourier transform and magnitude calculation. The experimental event sequence was controlled by a modular ICR data acquisition system.[27]

The AP/LIAD-CI FTICR mass spectrum of the base oil sample was internally calibrated with respect to a highly abundant homologous alkylation series.[28] Singly charged ions with relative abundance greater than six standard deviations of the baseline root-mean-square (rms) noise were exported to a spreadsheet, after identification of homologous series (i.e., species with the same $N_nO_oS_s$ content and number of rings plus double bonds, differing only by degree of alkylation) and peak assignment based on accurate mass and appropriate elemental constraints. For each elemental composition, $C_cH_hN_nO_oS_s$, the heteroatom class, type (double-bond equivalents, DBE, defined as the number of rings plus double bonds to carbon), and carbon number, c, were tabulated for generation of graphical DBE versus carbon number images.

FI TOF MS. The base oil sample was also analyzed with a Waters Micromas GCT Premier orthogonal acceleration time-of-flight (oa-TOF) mass spectrometer fitted with a field ionization (FI) source (Waters Corporation, Milford, MA, U.S.A.). The sample was deposited onto a capillary tube of a direct insertion probe and inserted into the FI source through a vacuum lock. The FI emitter (CarboTech, Gesellschaft fur instrumentelle Analytik mbH, Germany) consists of a 10 μm diameter tungsten wire onto which carbon microneedles have been grown. The emitter was set at ground potential with −12 kV applied to the extraction rods. The emitter current was set at 12 mA during scans and at 30 mA between scans to avoid sample deposition onto the emitter. For accurate mass measurement, chloropentafluorobenzene was used as a reference standard and introduced continuously into the ion source through a molecular leak. The molecular ion at 201.9609 Da was used as a lock mass during scans.

RESULTS AND DISCUSSION

Ion Source Optimization: Straight-Chain Alkanes. The performance of the new sample probe for analysis of saturated hydrocarbons was characterized and optimized by use of O_2 or N_2 as reagent gas. The reagent gas plays three main roles: (1) to serve as a carrier gas for entrainment of LIAD-vaporized analytes, which are directed toward the MS heated metal capillary (HMC) inlet, (2) to purge the region surrounding the MS inlet capillary of atmospheric gases, thereby controlling the ionization environment, and (3) to generate reactive species for chemical ionization. Supporting Information Figure S1 shows the effect of O_2 gas flow rate on the relative abundance of various reagent ions, based on scanning the low-mass range (m/z 15−200) of the linear ion trap, after initiation of corona discharge. In the absence of O_2 gas flow, the mass spectrum is dominated by $[(H_2O)_2 + H]^+$, originating from moisture in the ambient air surrounding the HMC inlet. Once the O_2 gas is turned on, the $O_2^{+\bullet}$ relative abundance increases sharply to become the dominant species, leveling off at flow rate >5 L/min, whereas $[(H_2O)_2 + H]^+$ decreases sharply to near zero due to depletion of moisture in the source region. The relative abundance of NO^+ increases slightly at 3.6 L/min O_2 gas flow rate, presumably due to an increased rate of reaction between O_2 and N_2 to generate NO^+, as the concentration of O_2 at the inlet capillary increases.[29] However, the NO^+ signal decreases to near zero at higher O_2 gas flow rate, following depletion of the ambient air N_2 by the high gas flow. The signal magnitudes for low-abundance background ions, N_2H^+ and H_3O^+, show little dependence on the O_2 gas flow rate. The use of N_2 as carrier/reagent gas exhibited similar behavior, except that N_2H^+ was the dominant species at high gas flow rate (>3.6 L/min, Supporting Information Figure S2) and $O_2^{+\bullet}$ was negligible.

AP/LIAD-CI MS optimization experiments for analysis of saturated hydrocarbons were performed by use of the straight-chain alkane, triacontane ($C_{30}H_{62}$). The carrier gas flow rate was the most critical ion source parameter that determined the abundance and distribution of analyte ions. No analyte signal was observed in the absence of carrier gas, presumably because the kinetic energy of the LIAD-vaporized neutrals is rapidly attenuated by collisions with atmospheric gases. The carrier gas thus serves to entrain the gas-phase analyte molecules toward the MS capillary inlet. Figure 2 shows mass spectra at each of four O_2 gas flow rates. At 1.8 L/min O_2, $[M - H]^+$ (hydride abstraction) dominates. Species corresponding to various

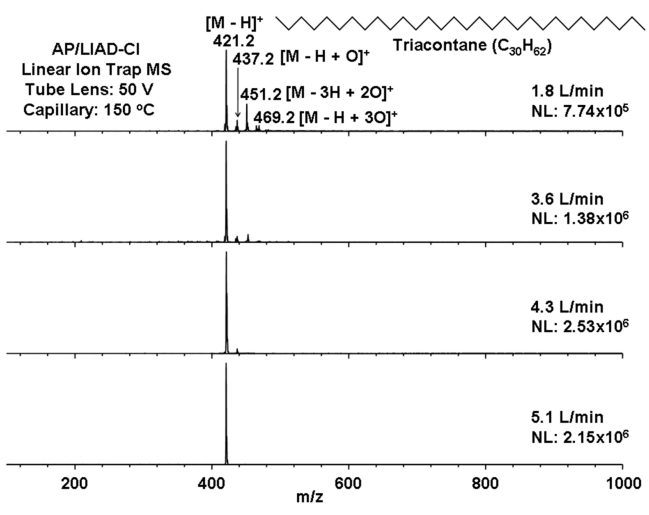

Figure 2. AP/LIAD-CI linear ion trap mass spectra for a straight-chain alkane (triacontane, $C_{30}H_{62}$) at each of several O_2 gas flow rates. The heated metal capillary was held at 150 °C and biased at 25 V, and the tube lens was biased at 50 V.

dx.doi.org/10.1021/ac301307p | Anal. Chem. 2012, 84, 7131−7137

degrees of oxidation (addition of up to four oxygen atoms) are also evident. The relative abundance of $[M - H]^+$ increases with O_2 gas flow rate, due to increased abundance of $O_2^{+\bullet}$ available for CI (see above). The magnitudes of the peaks that correspond to analyte oxidation decrease with increased O_2 gas flow rate and correlate with depletion of the ambient moisture in the cone−HMC interface. This observation suggests a role for atmospheric water in the generation of oxidation products, previously identified as hydrated analyte ions, e.g., $[M - 3H + H_2O]^+$ at m/z 437.2.[30,31] This assertion was verified by incorporation of $H_2{}^{18}O$ into the flow of O_2 carrier gas for AP/LIAD-CI analysis of triacontane ($C_{30}H_{62}$), by bubbling the gas through a vial containing 95 atom % ^{18}O-water (Sigma-Aldrich, St. Louis, MO, U.S.A.). This experiment was performed with a 9.4 T FTICR mass spectrometer to provide ultrahigh resolution ($m/\Delta m_{50\%}$ > 1 000 000 at m/z 400) and mass accuracy (<400 ppb) to unambiguously resolve and identify the signals. The mass spectrum shows an abundant signal for $[C_{30}H_{62} - H + {}^{18}O]^+$ that differs from $[{}^{12}C_{28}{}^{13}C_2H_{62} - H + O]^+$ by only 2.5 mDa (Supporting Information Figure S3). The relative abundance of $[C_{30}H_{62} - H + {}^{18}O]^+$ increases with the accumulation period which verifies that oxidation species are generated from hydration reactions. Alkane oxidation signals were minimized to less than 1% at 5.1 L/min O_2 gas flow rate, which was used for all subsequent experiments, for which $[M - H]^+$ is the main analyte ion detected, with no fragmentation, even if the capillary temperature is increased to 350 °C. However, minimal fragmentation does occur if the tube lens voltage is increased from 25 to 50 V and becomes significant at 75 V (Supporting Information Figure S4), an effect that could be exploited to provide structural information. Optimization of the cone-to-MS distance resulted in optimal signal magnitude at ∼5 mm. In general, the signal magnitude did not vary much (RSD = 25%) within the tested range (3−11 mm), indicating that the sample cone very efficiently confines the carrier gas/analyte stream moving toward the MS inlet. At the optimal ion source settings (carrier gas flow rate = 5.1 L/min, tube lens voltage = 25 V, capillary temperature = 150 °C, capillary voltage = 25 V, and cone-to-MS distance = 5 mm), the detection limit (S/N ≥ 3) determined by spotting serially diluted triacontane, based on experiments for a single MS acquisition, was 30 fmol.

Supporting Information Figure S5 identifies the analyte signals from use of O_2 versus N_2 as carrier/reagent gas, as clarified by 9.4 T FTICR mass-scale-expanded insets. $[M - H]^+$ is detected exclusively with O_2 as carrier gas (Supporting Information Figure S5, top). Similar results were obtained for tricosane ($C_{23}H_{48}$), nonacosane ($C_{29}H_{60}$), and hexatriacontane ($C_{36}H_{74}$, Supporting Information Figure S6), auguring for successful analysis of complex saturated hydrocarbon mixtures. With N_2 (Supporting Information Figure S5, bottom), the molecular ion, $M^{+\bullet}$, dominates the mass spectrum, with lower-abundance ion signals corresponding to losses of H and H_2, presumably from $M^{+\bullet}$, together with minor fragment ions. $M^{+\bullet}$ is generated by charge exchange with nitrogen radical cations[32] and undergoes some fragmentation due to the relatively larger difference in ionization energy between M and N_2 compared to O_2.[33]

Figure 3 shows a similar comparison between O_2 and N_2 carrier/reagent gas for a straight-chain alkane mixture (C_{21}−C_{40}). The mass spectra show nearly equal signal magnitudes for all of the alkanes in this range, as $[C_nH_{2n+2} - H]^+$ (n = 21−40), with somewhat more uniform ionization efficiency for O_2 (RSD

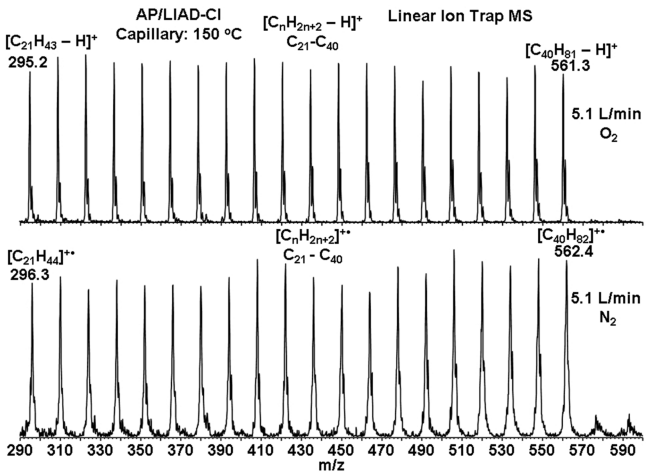

Figure 3. AP/LIAD-CI linear ion trap mass spectra for a mixture (40 μg/mL each) of straight-chain alkanes (C_{21}−C_{40}) for O_2 (top) or N_2 (bottom) carrier/reagent gas.

= 4.0%, Figure 3, top) than N_2 (RSD = 7.6%, Figure 3, bottom) carrier/reagent gas that yields $[C_nH_{2n+2}]^{+\bullet}$ species. The technique clearly holds promise for accurate relative quantitation for such mixtures. Moreover, the use of O_2 carrier gas yields overall 2.5-fold greater signal magnitude than N_2, presumably due to the lower ionization energy of O_2 (12.1 eV)[33] relative to N_2 (15.6 eV)[33] which results in greater number of reagent ions for more efficient CI. Paraffin mixtures ranging from C_{10} to C_{85} (m/z 140−1200) have been observed thus far by AP/LIAD-CI MS.

Branched Alkanes. The feasibility of AP/LIAD-CI MS for branched alkanes was tested by use of squalane ($C_{30}H_{62}$), an isomer of triacontane. Figure 4 shows the results for O_2 (top)

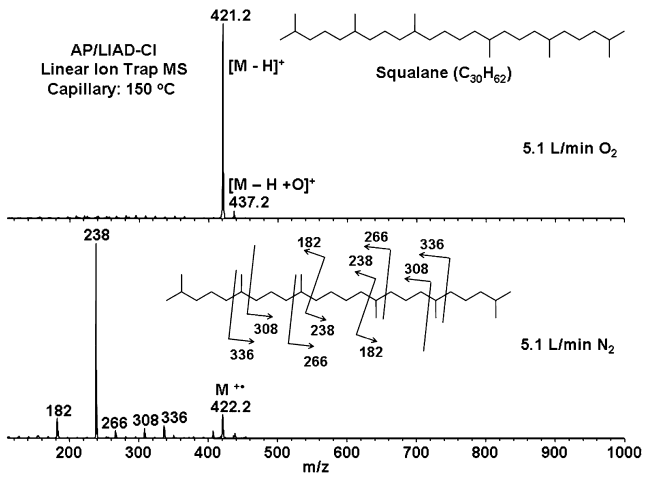

Figure 4. AP/LIAD-CI linear ion trap mass spectra for a branched alkane (squalane, $C_{30}H_{62}$) for O_2 (top) or N_2 (bottom) carrier/reagent gas.

and N_2 (bottom) carrier/reagent gas. With O_2, $[M - H]^+$ dominates the mass spectrum, with small peaks corresponding to fragment ions and $[M - H + O]^+$ (Figure 4, top). The relative abundance of the fragment ions increases slightly with increasing HMC temperature (Supporting Information Figure S7). In contrast, similar analysis by FI results in almost complete dissociation of the molecular ion.[8,34,35] AP/LIAD-CI with O_2 reagent gas thus offers a softer ionization approach for

dx.doi.org/10.1021/ac301307p | Anal. Chem. 2012, 84, 7131−7137

analysis of branched alkanes. With N_2 carrier/reagent gas, analyte fragment ions constitute the major peaks in the AP/LIAD-CI mass spectrum (Figure 4, bottom). The fragment ions are characteristic of collision-induced dissociation (CID), which generates highly stable tertiary carbocation fragments. The larger collisional cross section of squalane relative to its isomeric counterpart, triacontane, is responsible for its higher gas-phase reactivity and higher degree of fragmentation/oxidation. The ability of N_2 reagent gas to cause bond cleavages at the branching points could be useful for differentiating isomeric alkanes.

Cycloalkanes. The petroleum biomarker 5-α cholestane ($C_{27}H_{48}$) serves as a model compound to evaluate performance of the ion source for analysis of cycloalkanes. With O_2 as carrier/reagent gas, the analyte signal distribution depended on the temperature of the HMC (Figure 5). $M^{+\bullet}$ dominates the

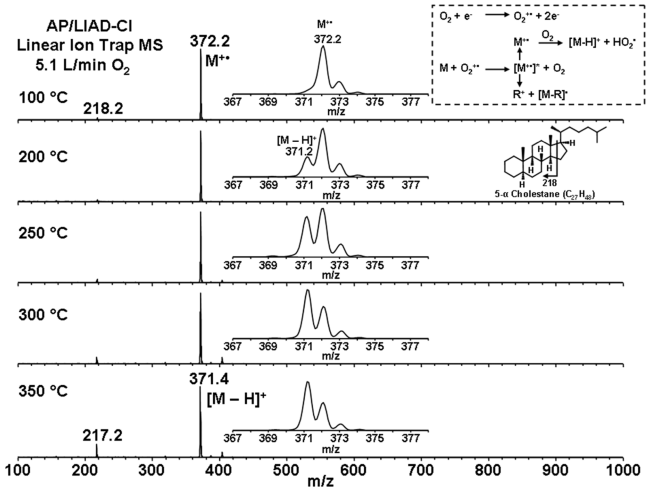

Figure 5. AP/LIAD-CI linear ion trap mass spectra for a cycloalkane (5-α cholestane $C_{27}H_{48}$) from corona discharge with O_2 carrier/reagent gas, at several heated metal capillary temperatures.

spectrum at HMC temperature below 100 °C, with a minute fragment ion signal at m/z 218.2 generated by cleavage across the D-ring of the sterane moiety[36] (Figure 5, top right). Above 100 °C, a peak corresponding to $[M - H]^+$ appears in the spectrum together with $M^{+\bullet}$. The abundance of $[M - H]^+$ increases relative to $M^{+\bullet}$ with increasing HMC temperature. $[M - H]^+$ becomes the main, intact analyte ion detected at HMC temperature above 350 °C. The analyte fragment ion also undergoes an m/z 218.2 to m/z 217.2 transition with increasing HMC temperature, due to loss of a hydrogen radical from the androstane moiety of the analyte. The magnitude of the fragment ion signal increases with increasing HMC temperature due to thermal activation of the precursor. Similar analyte ion distributions were observed with increasing O_2 carrier gas temperature: analytes are vaporized thermally by the heated gas in the absence of LIAD with the HMC held at 50 °C (Supporting Information Figure S8).

With N_2 carrier/reagent gas, $M^{+\bullet}$ dominates the spectrum, with no $[M - H]^+$ at any HMC temperature (100–350 °C, Supporting Information Figure S9), and the fragment ion does not lose hydrogen at high HMC temperature. The predominant pathway leading to hydride abstraction evidently requires O_2 and occurs in two steps. The data is consistent with an earlier proposed mechanism[37] that occurs via an $[M^{+\bullet}]^*$ transition state, generated in this case by thermal activation of $M^{+\bullet}$, which then reacts with O_2 by abstraction of a hydrogen atom according to the scheme in Figure 5, top right, in which R denotes alkyl chains.[37]

Polyethylene. A potential application of the present technique is determination of polyethylene molecular weight distribution and polydispersity. Results from analysis of two different polyethylenes (Polywax 500 and Polywax 655) by use of O_2 reagent/carrier gas with a linear ion trap and a 9.4 T FTICR mass spectrometer are summarized in Supporting Information Table S1. Supporting Information Figure S10 presents representative FTICR mass spectra of the two samples, showing a peak distribution corresponding to hydride abstraction from each polymer chain. The FTICR mass spectral results generally give weight-average (M_w) and number-average molecular weight (M_n) values somewhat higher than those obtained by GPC; the AP/LIAD-CI LIT MS values agree more closely with GPC data. The slightly higher values from AP/LIAD-CI FTICR MS could be due to time-of-flight mass discrimination that occurs as the ions are transmitted through the transfer quadrupole to the ICR cell. The time-of-flight effect can be corrected by acquisition of several mass spectra with incremental transfer period and the results superimposed on the same m/z axis.[38,39] However, high-resolution mass spectrometry facilitates identification of the polymer repeat units, thus complementing the GPC data.

Complex Saturated Hydrocarbon Mixture. Perhaps the most important application of this method is determination of the saturated hydrocarbon composition of crude oil fractions and similar mixtures for petroleum biomarker identification. However, facile and reliable determination of the identity of the various sample components requires coupling to high-resolution mass spectrometry to enable assignment of all observed ion signals. Initial analysis of a simple equimolar mixture of saturated hydrocarbons consisting of straight-chain (hexatriacontane), branched (squalane), and cycloalkane (5-α cholestane) generated analyte ion relative abundances of 100%, 89%, and 98%, indicating negligible ionization suppression for mixtures containing such species. Figure 6 shows results from analysis of a base oil sample by use of O_2 carrier/reagent gas with 9.4 T FTICR mass analysis. The mass spectrum contains more than 1700 assigned peaks (each with magnitude higher than 6σ of baseline noise) from m/z 159–700, mass resolving power ($m/\Delta m_{50\%}$, in which $\Delta m_{50\%}$ denotes the full mass spectral peak width at half-maximum peak height) of 600 000 at m/z 450, and 175 ppb rms error. The mass-scale-expanded inset (top, right) highlights the requirement for ultrahigh resolution to separate species that differ in elemental composition by ^{13}C versus CH (4.5 mDa difference in exact mass), for unambiguous assignment of elemental formulas for all of the peaks. The most abundant signals in the spectrum (highlighted by asterisks) correspond to a saturated hydrocarbon series (C_{12}–C_{49}).

Figure 6 (bottom) shows the isoabundance-contoured plot of DBE (DBE is the number of rings plus double bonds to carbon) versus carbon number for species with elemental compositions C_cH_h. The saturated hydrocarbon series (DBE = 0) corresponding to alkanes has the highest relative abundance for ions generated by hydride abstraction (Figure 6, bottom left). The figure also shows higher DBE series corresponding to cycloalkanes with increasing ring number (from one to eight rings). At an HMC temperature of ~250 °C, cycloalkanes also generate radical cations, as shown by an isoabundance-contoured plot of DBE versus carbon number (Figure 6,

dx.doi.org/10.1021/ac301307p | Anal. Chem. 2012, 84, 7131–7137

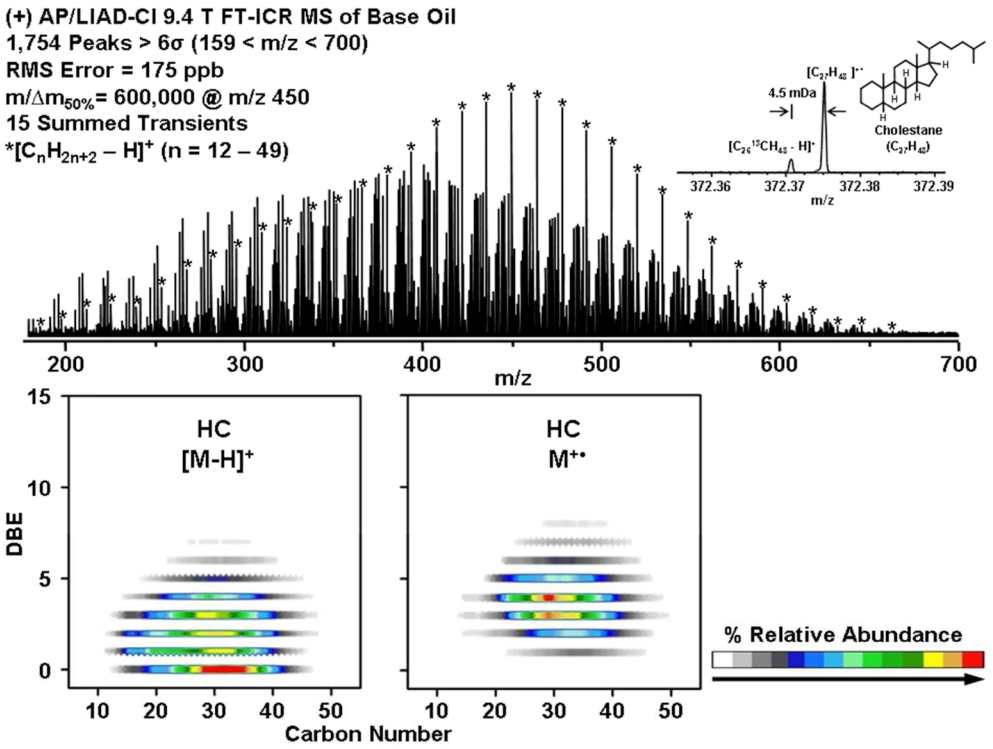

Figure 6. Top: AP/LIAD-CI 9.4 T FTICR mass spectrum for a base oil from a corona discharge in O_2 carrier/reagent gas. The mass-scale-expanded inset (top, right) highlights the requirement for ultrahigh resolution to separate species that differ in elemental composition by ^{13}C vs CH (4.5 mDa difference in exact mass). Bottom: isoabundance-contoured plot of double-bond equivalents vs carbon number for the hydrocarbon composition.

bottom right). High-abundance species with carbon number C_{27}–C_{30} and DBE = 4 likely represent C_{27}–C_{30} steranes, in agreement with GC/EIMS, GC × GC, and FIMS biomarker analysis of similar mixtures (Supporting Information Figure S11).[34,40] The assignment of C_{27} as cholestane, for example, is indicated by its expected hydride abstraction signal $[^{12}C_{26}{}^{13}C_1H_{48} - H]^+$, which differs in mass from the molecular ion by 4.5 mDa, as shown in the mass-scale-expanded inset (Figure 6, top right). The presence of hydride abstraction signals for the C_{28}–C_{30} steranes was also confirmed in the spectrum. The hopane series biomarkers, containing five rings (i.e., DBE = 5), are also apparent from the contour plot, which shows C_{29}–C_{35} as the most abundant species of that type (Figure 6, bottom left). Their corresponding $[M - H]^+$ signals are also confirmed in the spectrum and displayed in the left image.

Finally, Supporting Information Figure S12 shows an alternative presentation of the data as trend lines of relative abundance versus carbon number for each of the paraffin series, based on the number of rings (DBE) for each series. Because cycloparaffins generate $M^{+\bullet}$ and $[M - H]^+$ simultaneously (as noted above), their abundances were summed and then normalized (Supporting Information Figure S12). The data is in very good agreement with similar analysis by FI (Supporting Information Figure S11). The relative abundance for each paraffin series provides an estimate of its relative concentration for oil spill and oil contamination analyses. The sterane-to-hopane ratio has been used in petroleum exploration as a source facies indicator.[41]

CONCLUSIONS

We present AP/LIAD-CI MS with O_2 or N_2 carrier/reagent gas as a novel approach for saturated hydrocarbon mixture analysis. The carrier gas entrains the LIAD-vaporized analytes to the MS inlet, sweeps the region surrounding the inlet capillary free of atmospheric gases, and generates reagent ions for chemical ionization. With O_2 as carrier/reagent gas, $[M - H]^+$ species dominate the mass spectrum for straight-chain and branched alkanes, whereas cycloalkanes produce $[M - H]^+$ and $M^{+\bullet}$ at relative abundance determined by the temperature of the HMC. N_2 carrier/reagent gas produces predominantly $M^{+\bullet}$ for all alkane classes, but with significant fragmentation (at branching points) for branched alkanes to provide unique mass spectral fingerprints to distinguish constitutional isomers. Analysis of a straight-chain alkane mixture (C_{21}–C_{40}) with either O_2 or N_2 carrier/reagent gas provides comparable signal magnitude for all sample components. The present results are comparable to those previously reported by Campbell et al.[21,22] and Duan et al.[23] for analysis of saturated hydrocarbons by LIAD-CI MS with chemical ionization in vacuum by use of a cyclopentadienyl cobalt radical cation or ligated water cluster of Mn^+ ($ClMn(H_2O)^+$). However, the present AP/LIAD-CI provides similar results at atmospheric pressure for much higher throughput (less than 3 min per sample, including sample preparation). Operation at atmospheric pressure also enables accumulation of ions prior to mass analysis, for higher signal magnitude.

Combination of AP/LIAD-CI (O_2 carrier/reagent gas) with FTICR MS for analysis of complex hydrocarbon mixtures provides ultrahigh mass resolution and accuracy to enable unique and reliable assignment of elemental compositions. Analysis of a base oil sample by the present approach identifies more than 1700 elemental compositions (each derived from a mass spectral peak magnitude greater than 6σ of baseline rms noise) at mass resolving power of 600 000 at m/z 450 and rms mass error of 175 ppb from 15 time-domain acquisitions. The

dx.doi.org/10.1021/ac301307p | Anal. Chem. 2012, 84, 7131–7137

components consist of a paraffin (C_{12}–C_{49}) series and series of cycloparaffins containing one to eight rings, with relative abundances comparable to those produced by FI mass spectrometry.[34] However, AP/LIAD-CI MS provides a more economical and high-throughput alternative without the need to break vacuum for insertion of expensive FI/FD emitters (5–10 μm diameter) which are prone to break.

■ ASSOCIATED CONTENT

Supporting Information

Additional information as noted in text. This material is available free of charge via the Internet at http://pubs.acs.org.

■ AUTHOR INFORMATION

Corresponding Author

*Phone: +1 850-644-0529 (A.G.M.); +1 850-644-2398 (R.P.R.). Fax: +1 850-644-1366. E-mail: marshall@magnet.fsu.edu (A.G.M.); rodgers@magnet.fsu.edu (R.P.R.).

Notes

The authors declare no competing financial interest.

■ ACKNOWLEDGMENTS

This work was supported by NSF Division of Materials Research through DMR-06-54118, Florida State University Future Fuels Institute, and the State of Florida. The authors thank Daniel McIntosh for assistance with fabrication of the sample holder and Dr. Vladislav Lobodin for insightful discussions. Finally, we thank Chevron Energy Technology Co. for the FI-MS results.

■ REFERENCES

(1) Ludanyi, K.; Dallos, A.; Kuhn, Z.; Vekey, K. *J. Mass Spectrom.* **1999**, *34*, 264–267.
(2) Briker, Y.; Ring, Z.; Iacchelli, A.; McLean, N.; Rahimi, P. M.; Fairbridge, C.; Malhotra, R.; Coggiola, M. A.; Young, S. E. *Energy Fuels* **2001**, *15*, 23–37.
(3) Qian, K.; Dechert, G. J. *Anal. Chem.* **2002**, *74*, 3977–3983.
(4) Schaub, T. M.; Hendrickson, C. L.; Qian, K.; Quinn, J. P.; Marshall, A. G. *Anal. Chem.* **2003**, *75*, 2172–2176.
(5) Amirav, A.; Gordin, A.; Tzanani, N. *Rapid Commun. Mass Spectrom.* **2001**, *15*, 811–820.
(6) Dagan, S.; Amirav, A. *J. Am. Soc. Mass Spectrom.* **1995**, *6*, 120–131.
(7) Nir, E.; Hunziker, H. E.; de Vries, M. S. *Anal. Chem.* **1999**, *71*, 1674–1678.
(8) Hsu, C. S.; Blum, S. C.; Liang, Z.; Grosshans, P. B.; Robbins, W. K. U.S. Patent 5,644,129, July 1, 1997.
(9) Chen, R.; Li, L. *J. Am. Soc. Mass Spectrom.* **2001**, *12*, 367–375.
(10) Chen, R.; Yalcin, T.; Wallace, W. E.; Guttman, C. M.; Li, L. *J. Am. Soc. Mass Spectrom.* **2001**, *12*, 1186–1192.
(11) Cody, R. B. *Anal. Chem.* **2009**, *81*, 1101–1107.
(12) Yang, Z. H.; Attygalle, A. B. *J. Am. Soc. Mass Spectrom.* **2011**, *22*, 1395–1402.
(13) Wu, C. P.; Qian, K. N.; Nefliu, M.; Cooks, R. G. *J. Am. Soc. Mass Spectrom.* **2010**, *21*, 261–267.
(14) Gao, J. S.; Owen, B. C.; Borton, D. J.; Jin, Z. C.; Kenttamaa, H. I. *J. Am. Soc. Mass Spectrom.* **2012**, *23*, 816–822.
(15) Hourani, N.; Kuhnert, N. *Anal. Methods* **2012**, *4*, 730–735.
(16) Golovlev, V. V.; Allman, S. L.; Garrett, W. R.; Chen, C. H. *Appl. Phys. Lett.* **1997**, *71*, 852–854.
(17) Golovlev, V. V.; Allman, S. L.; Garrett, W. R.; Taranenko, N. I.; Chen, C. H. *Int. J. Mass Spectrom.* **1997**, *169*, 69–78.
(18) Lindner, B.; Seydel, U. *Anal. Chem.* **1985**, *57*, 895–899.
(19) Perez, J.; Ramirez-Arizmendi, L. E.; Petzold, C. J.; Guler, L. P.; Nelson, E. D.; Kenttamaa, H. I. *Int. J. Mass Spectrom.* **2000**, *198*, 173–188.
(20) Shea, R. C.; Petzold, C. J.; Liu, J.-A.; Kenttaemaa, H. I. *Anal. Chem.* **2007**, *79*, 1825–1832.
(21) Campbell, J. L.; Crawford, K. E.; Kenttaemaa, H. I. *Anal. Chem.* **2004**, *76*, 959–963.
(22) Campbell, J. L.; Fiddler, M. N.; Crawford, K. E.; Gqamana, P. P.; Kenttaemaa, H. I. *Anal. Chem.* **2005**, *77*, 4020–4026.
(23) Duan, P.; Qian, K.; Habicht, S. C.; Pinkston, D. S.; Fu, M.; Kenttaemaa, H. I. *Anal. Chem.* **2008**, *80*, 1847–1853.
(24) Jia, L. Y.; Weng, J. J.; Zhou, Z. Y.; Qi, F.; Guo, W. Y.; Zhao, L. M.; Chen, J. *Rev. Sci. Instrum.* **2012**, *83*, 026105.
(25) Nyadong, L.; McKenna, A. M.; Hendrickson, C. L.; Rodgers, R. P.; Marshall, A. G. *Anal. Chem.* **2011**, *83*, 1616–1623.
(26) Kaiser, N. K.; Savory, J. J.; McKenna, A. M.; Quinn, J. P.; Hendrickson, C. L.; Marshall, A. G. *Anal. Chem.* **2011**, *83*, 6907–6910.
(27) Blakney, G. T.; Hendrickson, C. L.; Marshall, A. G. *Int. J. Mass Spectrom.* **2011**, *306*, 246–252.
(28) Qian, K.; Robbins, W. K.; Hughey, C. A.; Cooper, H. J.; Rodgers, R. P.; Marshall, A. G. *Energy Fuels* **2001**, *15*, 1505–1511.
(29) Ono, R.; Tobaru, C.; Teramoto, Y.; Oda, T. *Plasma Sources Sci. Technol.* **2009**, *18*, 025006/025001–025006/025007.
(30) Bell, S. E.; Ewing, R. G.; Eiceman, G. A.; Karpas, Z. *J. Am. Soc. Mass Spectrom.* **1994**, *5*, 177–185.
(31) Borsdorf, H.; Nazarov, E. G.; Eiceman, G. A. *J. Am. Soc. Mass Spectrom.* **2002**, *13*, 1078–1087.
(32) Huang, S. *Org. Mass Spectrom.* **1989**, *24*, 1065–1071.
(33) NIST Chemistry WebBook, accessed 11/1/2011. http://webbook.nist.gov/chemistry/name-ser.html.
(34) Hsu, C. S. *Prepr. Symp.—Am. Chem. Soc., Div. Fuel Chem.* **2011**, *56*, 421.
(35) Liang, Z.; Hsu, C. S. *Energy Fuels* **1998**, *12*, 637–643.
(36) Wang, G.; Zhang, L.; Wang, T. *Chin. Sci. Bull.* **2006**, *51*, 1628–1632.
(37) Marotta, E.; Paradisi, C. *J. Am. Soc. Mass Spectrom.* **2009**, *20*, 697–707.
(38) Dey, M.; Castoro, J. A.; Wilkins, C. L. *Anal. Chem.* **1995**, *67*, 1575–1579.
(39) O'Connor, P. B.; Duursma, M. C.; van Rooij, G. J.; Heeren, R. M. A.; Boon, J. J. *Anal. Chem.* **1997**, *69*, 2751–2755.
(40) Juyal, P.; McKenna, A. M.; Yen, A.; Rodgers, R. P.; Reddy, C. M.; Nelson, R. K.; Andrews, A. B.; Atolia, E.; Allenson, S. J.; Mullins, O. C.; Marshall, A. G. *Energy Fuels* **2011**, *25*, 172–182.
(41) Hsu, C. S.; Walters, C. C.; Isaksen, G. H.; Schaps, M. E.; Peters, K. E. *Analytical Advances for Hydrocarbon Research*; Kluwer Academic/Plenum Publishers: New York, 2003; pp 223–245.